Dominant spectra of background radiation in an SF6 post-arc channel

Dominant Spectra of Background Radiation in an SF_6 Post-Arc Channel

Yasunori Tanaka, Yasunobu Yokomizu, *Member, IEEE*, Motohiro Ishikawa, Toshiro Matsumura, *Member, IEEE*, and Yukio Kito, *Fellow, IEEE*

***Abstract*—Composition of background spectra radiated from an SF_6 post-arc channel after current zero was investigated. The radiation intensity of background spectra at a wavelength of 455 nm around current zero was measured. Post-arc temperature was estimated from the intensity ratio of two spectral lines at 426.0 and 442.7 nm of iron used as an electrode material. Emission coefficients of not only continuous spectra but also S_2 spectra due to $B^3\Sigma_u^- - X^3\Sigma_g^-$ transition were theoretically calculated as a function of temperature in the range of 3000–6000 K. The results indicated that the background spectra mainly consist of continuous spectra at temperatures above 4500 K, and of S_2 spectra at temperatures below 4500 K. The temperature dependence of the calculated emission coefficients of the background spectra agreed fairly well with that of the measured radiation intensity.**

***Index Terms*—Background radiation, continuous spectra, S_2 spectra, SF_6 post-arc channel.**

I. Introduction

In an SF_6 gas-blast circuit breaker, an arc discharge was established between the electrodes during current interruption processes. In order to elucidate the arc interruption phenomena, diagnosis of the arc temperature T and concentration X_M of metallic vapor ejected from the electrodes into the arc is of great importance. In measuring T and X_M in the arc column, spectroscopic observation is often performed to observe not only objective spectral lines but also background spectra near these spectral lines. Thus, it is necessary to investigate the background spectra. The background spectra at $T > 6000$ K is usually considered to be continuous spectra. Until now, several studies have been done to find out various properties of the continuous spectra at $T > 6000$ K [1], [2].

On the other hand, temperature of post-arc channel after current zero decays to magnitudes below 6000 K. However, very little is known about the continuous spectra at $T < 6000$ K. In addition, there are few studies on the composition of the background spectra at $T < 6000$ K.

The present paper describes the background spectra radiated from an SF_6 post-arc channel. First, time variation of radiation intensity I_{455} of background spectra at a wavelength of 455 nm was measured around current zero in a flat-type SF_6 gas-blast quenching chamber. In the chamber, we intentionally used iron electrodes, and observed Fe spectral lines at wavelengths of 426.0 and 442.7 nm together with the background spectra. This is because these Fe spectral lines have much higher radiation intensities than those of S^+, F, or Cu at $T < 6000$ K [3], [4]. Application of the two-line method to the measured two Fe spectral lines enabled us to estimate the post-arc temperature T up to 100 μs after current zero for ac 5 kA_{peak} arcs [3], [4]. As a result, the radiation intensity I_{455} of the observed background spectra was successfully obtained as a function of T. Second, to interpret the temperature dependence of I_{455}, integrated emission coefficient ε'_{cont} of the continuous spectra at 455 nm was theoretically calculated as a function of T in the range from 3000 to 6000 K. However, the temperature dependence of ε'_{cont} shows no agreement with that of the observed I_{455}. Finally, special attention was given to molecular spectra, where the integrated emission coefficient $\varepsilon_{S_2 455}$ of S_2 spectra due to $B^3\Sigma_u^- - X^3\Sigma_g^-$ transition has to be taken into account for the background spectra at $T < 6000$ K, since the temperature dependence of the sum of $\varepsilon_{S_2 455}$ and ε'_{cont} agrees fairly well with that of I_{455}.

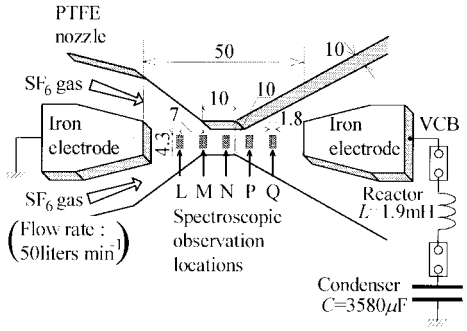

Fig. 1. Flat-type SF_6 gas-blast quenching chamber and spectroscopic observation position.

II. Measurement of Radiation Intensities of Iron Spectral Lines and Background Spectra

A. Experimental Setup

Fig. 1 depicts the flat-type SF_6 gas-blast quenching chamber adopted in the experiment [3], [4]. In this chamber, we intentionally used two iron electrodes. A flat nozzle is made of polytetrafluoroethylene (PTFE) with a thickness of 10 mm. The nozzle throat is 10 mm wide and 10 mm long. The flat nozzle was sandwiched between two ceramic plates.

Manuscript received November 25, 1996; revised January 27, 1997. This work was supported by Grant-in-Aid for Scientific Research (A)(2) 08555068.

Y. Tanaka, Y. Yokomizu, M. Ishikawa, and T. Matsumura are with the Department of Electrical Engineering, Nagoya University, Furo-cho, Chikusa-ku, Nagoya, Aichi 464-01, Japan (e-mail: tanaka@matsumura.nuee.nagoya-u.ac.jp).

Y. Kito is with the Toyota National College of Technology, 2-1, Eisei-cho, Toyota, Aichi 471, Japan.

Publisher Item Identifier S 0093-3813(97)07236-6.

Sulfur hexafluoride gas was supplied through tubes along the cathode to blow in the axial direction to the arc. The flow rate was adjusted to 50 l/min^{-1} before arc ignition. Gas pressure in the chamber was always kept to be nearly 0.1 MPa.

A damping sinusoidal current with a frequency of 60 Hz was supplied from a capacitor bank (with capacitance C of 3580 μF) through a reactor (with inductance L of 1.9 mH). Peak value of the current was adjusted to 5000 A. An auxiliary vaccum circuit breaker (VCB) was intentionally connected in series with this flat-type quenching chamber, thus interrupting the sinusoidal current at the first current zero. As a result, no transient recovery voltage (TRV) was applied between the electrodes in the flat-type quenching chamber.

B. Spectroscopic Observation Along Nozzle Axis

Spectroscopic observation was carried out at five positions around the nozzle throat as denoted by the symbol L–Q in Fig. 1. At these positions, the ceramic plate sandwiching the flat nozzle has a rectangular hole of 4 mm × 1 mm. Through this hole, the arc radiation was observed with a bundle of four optical fibers made of quartz glass. Each fiber has a core of 0.8 mm in diameter, a clad of 1.0 mm in diameter, and a numerical aperture of 0.2. The bundle of fibers accepts arc radiation from a region with spatial dimensions of 4.3 mm × 1.8 mm.

This bundle of fibers transmits the arc radiation from the observation point to the entrance slit of a monochromator. The monochromator has a reciprocal dispersion of 0.8 nm · mm^{-1}. On the focal plane at the exit of the monochromator, a multichannel detector with three photomultiplier tubes was positioned. Use of this detector permits the simultaneous observation of radiation intensities at three different wavelengths. With the multichannel detector, we measured the radiation intensities I'_{426} and I'_{443} at wavelengths of 426.0 and 442.7 nm, respectively. Simultaneously, the radiation intensity I_{455} at a wavelength of 455.0 nm was also measured to obtain the intensity of background spectra. The wavelength of 455.0 nm is free from the spectral lines emitted from atoms and atomic ions. The observation width of each channel corresponds to 0.6 nm in wavelength. The relative spectral sensitivities of the overall optical system for the above three wavelengths were measured using a standard tungsten-halide lamp. Considering the sensitivities thus obtained, corrections were made to the three signals.

C. Time Variations of Radiation Intensities of Spectra and Temperature around Current Zero

Numerical subtraction of background radiation intensity I_{455} from I'_{426} produces the net radiation intensity I_{Fe426} of Fe spectral line at 426.0 nm $(z^7\mathrm{D^o}\text{-}e^7\mathrm{D})$. Similarly, the net radiation intensity I_{Fe443} of Fe spectral line at 442.7 nm $(a^5\mathrm{D}\text{-}z^7\mathrm{F^o})$ was also derived. The top part of Fig. 2 illustrates the time variations of radiation intensities $I_{\mathrm{Fe426}}, I_{\mathrm{Fe443}}$, and I_{455} at position M. As can be seen in this figure, all of $I_{\mathrm{Fe426}}, I_{\mathrm{Fe443}}$, and I_{455} were detectable up to 100 μs after current zero. It should be noted that I_{Fe426} and I_{Fe443} decay rapidly with time, while I_{455} of the background spectra almost remain constant. A similar aspect was found at the other observation positions.

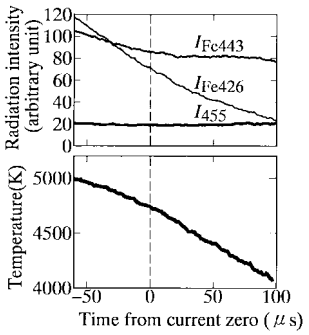

Fig. 2. Time variations of radiation intensity measured around current zero and temperature estimated at position M (Peak value of current, 5 kA; SF_6 gas flow rate, 50 l/min).

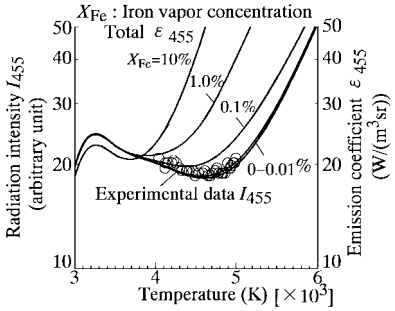

Fig. 3. Temperature dependence of the radiation intensity of background spectra at 455 nm measured at position M and those of emission coefficients calculated.

From the ratio $I_{\mathrm{Fe443}}/I_{\mathrm{Fe426}}$, temperature T around current zero was estimated by the two-line method on the assumption that the population of excited states in Fe follows a Boltzmann distribution and that the arc is optically thin. The validity of these assumptions was confirmed in additional experiments by measuring simultaneously Fe spectral lines at 430.8, 432.6, 438.6, 440.5, and 441.5 nm, as well as at 426.0 and 442.7 nm with an optical multichannel analyzer and by making a Boltzmann plot diagram for the seven lines. The bottom figure in Fig. 2 represents the decay process of T at the position M. Note that T is so-called an excitation temperature of Fe. The temperature T was estimated to be 4870 K at the current zero. It can be also seen that T decreases gradually with time, then reaching to 4140 K at 100 μs after current zero.

III. Temperature Dependence of Radiation Intensity of Background Spectra

Use of Fig. 2 permits us to obtain I_{455} as a function of T. Open circles in Fig. 3 designate I_{455} as a function of T. The intensity I_{455} decreases with T from 5000 to 4600 K, while I_{455} increases slightly with a reduction of T from 4600 to 4100 K. In order to interpret the above relationship between I_{455} and T, emission coefficient ε_{455} of background spectra at 455 nm will be discussed in the next section.

IV. Theoretical Calculation of Emission Coefficients of Background Spectra

A. Equilibrium Composition of SF_6–Fe Mixture Plasma

The calculations of emission coefficients require the particle composition of SF_6–Fe mixture. Thus, we calculated the equilibrium composition of SF_6 gas contaminated with iron vapor [3], [4]. The species taken into account were the molecular, atomic, and ionic species of SF_6, SF_4, SF_2, F_2, S_2 F, S, F^+, S^+, F^-, S^-, F^{2+}, S^{2+}, Fe, Fe^+, Fe^{2+}, and electron. We obtained the composition by solving the simultaneous equations: Saha's equation for ionization reactions, Gulberg–Waage's equations for dissociation reactions, the charge neutrality equation, Dalton's laws of partial pressures, and the equation defining the iron vapor concentration $X_{\rm Fe}$. In the present paper, $X_{\rm Fe}$ (in %) is defined as the ratio of the total mass of Fe, Fe^+, and Fe^{2+} to the sum of those of all particles:

$$X_{\rm Fe} = \frac{m_{\rm Fe}(N_{\rm Fe} + N_{\rm Fe^+} + N_{\rm Fe^{2+}})}{\sum_j m_j N_j} \times 100. \tag{1}$$

B. Emission Coefficient of Continuous Spectra

Background spectra are usually considered to be continuous spectra, especially at $T > 6000$ K. Thus, we calculated the emission coefficient of the continuous spectra taking into account four kinds of radiative mechanisms: 1) recombination radiation, 2) radiation by electron attachment, 3) bremsstrahlung, and 4) radiation by collision between electron and neutral species [5].

1) Recombination Radiation: The emission coefficient $\varepsilon_{\rm fb}$ (in $\rm W \cdot m^{-4} \cdot sr^{-1}$) of the continuous spectra due to recombination at a wavelength of λ is given by

$$\varepsilon_{\rm fb} = C_1 \frac{N_e}{T^{1/2}} \left[1 - \exp\left(-\frac{hc}{kT\lambda}\right)\right] \times \sum_{j({\rm ion})} \frac{g_{1j} Z_{{\rm eff}\,j}^2 N_j}{U_j} \xi_j \frac{c}{\lambda^2}$$
$$C_1 = \frac{1}{(4\pi\varepsilon_0)^3} \frac{16\pi e^6}{3c^3(6\pi m_e^3 k)^{1/2}} \tag{2}$$

where e the electronic charge, m_e the mass of electron, h Planck's constant, c the velocity of light, k Boltzmann's constant, g_{1j} the statistical weight of the ground state of species j, and U_j the internal partition function of species j. The quantities N_e and N_j are the number density of the electron and the species j, respectively, $Z_{{\rm eff}\,j}$ is the effective ionic charge of the species j, and ξ_j is the Bibermann–Schlüter factor for nonhydrogenic particles [6]. The wavelength λ was taken to be 455.0 nm.

2) Radiation by Electron Attachment: Atoms such as F and S can capture a free electron to form negative ions F^- and S^- with the emission of a continuum similar to that of the recombination process. However, the attachment continuum of F^- occurs at $\lambda < 364.6$ nm because of the existence of the absorption edges [7], while that of S^- at $\lambda < 614.4$ nm [8]. Thus, the electron attachment to S mainly contributes to the light emission at 455.0 nm. The emission coefficient $\varepsilon_{\rm attach}$ of the light at λ is expressed as

$$\varepsilon_{\rm attach} = \frac{2hc}{\lambda^3} \exp\left(-\frac{hc}{kT\lambda}\right) N_{\rm S^-} \sigma_{\rm det}^{\rm S^-} \frac{c}{\lambda^2} \tag{3}$$

where $N_{\rm S^-}$ is the number density of S^-, $\sigma_{\rm det}^{\rm S^-}$ is the photodetachment cross sections for S^-.

3) Bremsstrahlung: The emission coefficient $\varepsilon_{\rm ff}$ of the continuous spectra due to free–free transitions of electrons can be calculated by the following equation:

$$\varepsilon_{\rm ff} = C_1 \frac{N_e}{T^{1/2}} \exp\left(-\frac{hc}{kT\lambda}\right) \times \sum_{j({\rm ion})} Z_{{\rm eff}\,j}^2 N_j G_{\rm ff} \frac{c}{\lambda^2} \tag{4}$$

where $G_{\rm ff}$ is the temperature-averaged free–free Gaunt factor, which is close to unity [9].

4) Radiation by Collision Between Electron and Neutral Species: The emission coefficient $\varepsilon_{\rm en}$ of continuum due to collisions between electron and neutral particles is given as follows [5]:

$$\varepsilon_{\rm en} = \frac{32e^2}{3c^3(4\pi\varepsilon_0)} \left(\frac{kT}{2\pi m_e}\right)^{3/2} N_e \exp\left(-\frac{hc}{kT\lambda}\right) \times \sum_{j({\rm neutral})} N_j G_{{\rm n}j} \frac{c}{\lambda^2} \tag{5}$$

where $G_{{\rm n}j}$ is a factor depending on the cross sections of elastic electron–neutral collision.

The calculation results revealed that $\varepsilon_{\rm attach}$ is very much higher than $\varepsilon_{\rm fb}, \varepsilon_{\rm ff}$, and $\varepsilon_{\rm en}$ in the temperature range from 3000 to 6000 K. For example, at $T = 5000$ K, $\varepsilon_{\rm attach}$ is more than 130 times greater than those by the other three processes.

The summation of $\varepsilon_{\rm fb}, \varepsilon_{\rm attach}, \varepsilon_{\rm ff}$, and $\varepsilon_{\rm en}$ yields the total emission coefficient $\varepsilon_{\rm cont}$ of the continuous spectra

$$\varepsilon_{\rm cont} = \varepsilon_{\rm fb} + \varepsilon_{\rm attach} + \varepsilon_{\rm ff} + \varepsilon_{\rm en}. \tag{6}$$

Fig. 4 indicates $\varepsilon_{\rm cont}$ as a function of T in the range of 3000–6000 K at $P = 0.1$ MPa with a parameter of $X_{\rm Fe}$. As seen in this figure, $\varepsilon_{\rm cont}$ decreases markedly with reducing T for the same $X_{\rm Fe}$.

The measured I_{455} included radiation intensities integrated in wavelength range of 455.0 ± 0.3 nm. Thus, we calculated

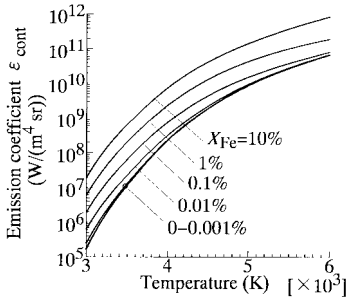

Fig. 4. Emission coefficient $\varepsilon_{\rm cont}$ of continuous spectra at a wavelength of 455.0 nm in SF_6 gas at 0.1 MPa as a function of temperature.

the integrated emission coefficient $\varepsilon'_{\rm cont}$ (in $\rm W\cdot m^{-3}\cdot sr^{-1}$) of continuum in the range of 455.0 ± 0.3 nm by

$$\varepsilon'_{\rm cont} = \int_{454.7\rm nm}^{455.3\rm nm} \varepsilon_{\rm cont}\, d\lambda \simeq \varepsilon_{\rm cont} \times (0.6\ \rm nm). \qquad (7)$$

Although not being able to compare values of I_{455} with the absolute values of $\varepsilon'_{\rm cont}$, we are able to compare the temperature dependence of I_{455} with that of $\varepsilon'_{\rm cont}$, i.e., that of $\varepsilon_{\rm cont}$. It should be noted that the temperature dependence of $\varepsilon_{\rm cont}$ greatly differs from that of I_{455} shown with the open circles in Fig. 3. This result indicates that background spectra include significant spectra besides the continuous spectra in the temperature range of 3000–6000 K.

C. Emission Coefficient of S_2 Spectra Due to $B^3\Sigma_u^- – X^3\Sigma_g^-$ Transition

In the temperature range of 3000–6000 K, the high-temperature SF_6 gas has the molecules such as S_2, F_2, and SF_2. Thus, particular attention to the molecular spectra was paid especially to S_2 spectra. The reasons are given below. 1) SF_2 has much lower number density than S_2. 2) F_2 emits band spectra with marked low intensity, because F_2 has much higher electronic energy of upper state than S_2 [10].

Sulfur molecules S_2 emit very extensive band spectra mainly through $B^3\Sigma_u^- – X^3\Sigma_g^-$ transition [11]. The emission coefficient ε_{S_2} (in $\rm W\cdot m^{-3}\cdot sr^{-1}$) for $B^3\Sigma_u^- – X^3\Sigma_g^-$ transition of S_2 is written by

$$\varepsilon_{S_2} = \frac{hc}{4\pi\lambda_{v'v''J'J''}} N_{n'v'J'} A_{v'v''J'J''} \qquad (8)$$

where n, v, J are the quantum numbers on electronic, vibrational, and rotational state, respectively. The prime ($'$) denotes the upper state, and the double prime ($''$) the lower state. Then, $\lambda_{v'v''J'J''}$ is the wavelength, and $A_{v'v''J'J''}$ the transition probability. The calculation was performed for vibrational transitions $(v', v'') = (0,0), (0,1), \cdots, (12,25), (12,26)$ and for rotational transitions including P and R branches with $J' = 0, \cdots, 500$. Fig. 5 represents ε_{S_2} at $P = 0.1$ MPa as a function of wavelength at $T = 4000$ K. This figure reveals that S_2 has differences of 9% in emission coefficients at the wavelengths of 426.0, 442.7, and 455.0 nm. This difference may cause an error in temperature estimates. However, the error is only 20 K at current zero in Fig. 2 for example. Thus, emission coefficient of S_2 at 455.0 nm can be regarded as background spectra at the three wavelengths.

The integrated emission coefficient $\varepsilon_{S_2 455}$ in the wavelength range of 455.0 ± 0.3 nm was expressed as follows:

$$\varepsilon_{S_2 455} = \sum_{455.0\pm0.3\ \rm nm} \varepsilon_{S_2}. \qquad (9)$$

Fig. 6 represents $\varepsilon_{S_2 455}$ as a function of T for $X_{\rm Fe}$ from 0 to 10%. As can be seen in this figure, $\varepsilon_{S_2 455}$ increases gradually with reducing T. For example, $\varepsilon_{S_2 455}$ has the magnitude of 10.8 $\rm W\cdot m^{-3}\cdot sr^{-1}$ at 6000 K, while $\varepsilon_{S_2 455}$ is 19.8 $\rm W\cdot m^{-3}\cdot sr^{-1}$ at 3000 K. From Fig. 6, $\varepsilon_{S_2 455}$ is also found to be almost independent of $X_{\rm Fe}$ in range of 0–1% for a given T.

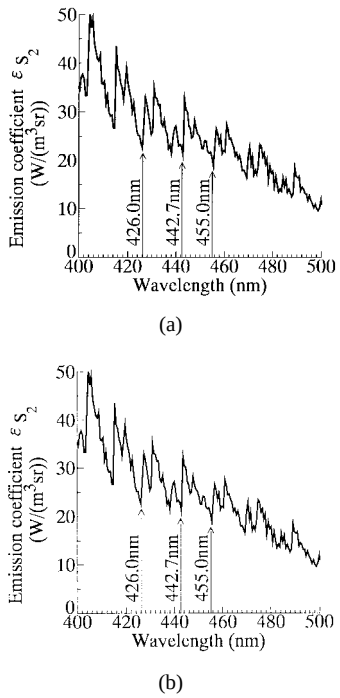

Fig. 5. Dependence of emission coefficient due to S_2 $B^3\Sigma_u^- - X^3\Sigma_g^-$ transition on wavelength in pure SF_6 gas at 4000 K at 0.1 MPa.

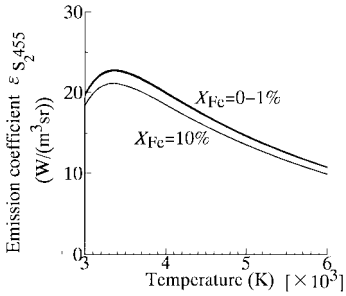

Fig. 6. Emission coefficient due to $S_2 B^3\Sigma_u^- - X^3\Sigma_g^-$ transition in wavelength range from 454.7 to 455.3 nm in SF_6 gas at 0.1 MPa as a function of temperature.

V. Comparison of Calculated Emission Coefficient with Measured Radiation Intensity of Background Spectra

Let us calculate total integrated emission coefficient ε_{455} of background spectra in the range of 455.0 ± 0.3 nm:

$$\varepsilon_{455} = \varepsilon'_{\rm cont} + \varepsilon_{S_2 455}. \qquad (10)$$

In Fig. 3, bold curves represent ε_{455} as a function of T at $P = 0.1$ MPa. It should be noted that the temperature dependence of ε_{455} for $X_{\rm Fe} = 0$–0.01% agrees fairly well with that of I_{455}. This agreement indicates that the background spectra at the wavelength of 455 nm mainly consist of not continuous spectra but S_2S_2 spectra through $B^3\Sigma_u^- - X^3\Sigma_g^-$ transition at $T < 4500$ K. In addition, the agreement also suggests that $X_{\rm Fe}$ in the post-arc channel was probably of order of 0–0.01%.

VI. Conclusions

We investigated background spectra in an SF_6 post-arc channel after current zero. Spectroscopic observations were performed to obtain radiation intensity I_{455} of the background spectra at 455 nm as a function of temperature T. The intensity I_{455} proved to decrease with T from 5000 to 4600 K, while to increase slightly with T from 4600 to 4100 K. To interpret the aspect of this temperature dependence, we first calculated emission coefficient $\varepsilon_{\rm cont}$ of continuous spectra in the temperature range of 3000–6000 K. However, the temperature dependence of $\varepsilon_{\rm cont}$ shows no agreement with that of I_{455} in the temperature range from 3000 to 5000 K. The emission coefficient ε_{S_2455} of S_2 spectra due to $B^3\Sigma_u^- - X^3\Sigma_g^-$ transition at 455 nm were theoretically calculated as a function of T. Then, we derived the emission coefficient ε_{455} of background spectra by summing ε_{S_2455} and $\varepsilon'_{\rm cont}$ at 455 nm. The temperature dependence of ε_{455} agreed fairly well with that of I_{455}. This result indicates that the background spectra mainly consist of continuous spectra at $T > 4500$ K, while of S_2 spectra at $T < 4500$ K.

References

[1] A. Sola, M. D. Calzada, and A. Gamero, "On the use of the line-to continuum intensity ratio for determining the electron temperature in a high-pressure argon surface-microwave discharge," *J. Phys. D, Appl. Phys.*, vol. 28, pp. 1099–1110, 1995.

[2] H. R. Griem, *Plasma Spectroscopy*. New York: McGraw-Hill, 1964, pp. 279–283.

[3] Y. Tanaka, Y. Yokomizu, T. Matsumura, and Y. Kito, "Transient behavior of axial temperature distribution in post-arc channel after current zero around nozzle throat in flat-type SF_6 gas-blast quenching chamber," *J. Phys. D, Appl. Phys.*, vol. 28, pp. 2095–2103, 1995.

[4] ——, "Transient distribution of metallic vapor concentration in a post-arc channel after current zero along the nozzle axis in a flat-type SF_6 gas-blast quenching chamber," *J. Phys. D, Appl. Phys.*, vol. 29, pp. 1540–1550, 1996.

[5] F. Cabannes and J. Chapelle, *Reactions under Plasma Conditions*. New York: Wiley, 1971, vol. 1, ch. 7.

[6] L. M. Bibermann and G. E. Norman, "On the calculation of photoionization absorption," *Opt. Spectrosc.*, vol. 8, pp. 230–232, 1960.

[7] A. Mandl, "Electron photodetachment cross section of the negative iron of fluorine," *Phys. Rev. A*, vol. 3, pp. 251–255, 1971.

[8] W. C. Lineberger and B. W. Woodward, "High resolution phtodetachment of S^- near threshold," *Phys. Rev. Lett.*, vol. 25, pp. 424–427, 1970.

[9] H. Kafrouni and S. Vacquie, "Study of the recombination continuum an SF_6 arc discharge," *J. Quant. Spectrosc. Radiat. Transf.*, vol. 32, pp. 219–224, 1984.

[10] G. Herzberg, *Molecular Spectra and Molecular Structure IV. Constants of Diatomic Molecules*. New York: Litton, 1979.

[11] R. W. B. Pearse and A. G. Gaydon, *The Identification of Molecular Spectra*. New York: Wiley, 1976.

Yasunori Tanaka was born in Mie, Japan, on November 19, 1970. He received the B.S. and M.S. degrees in electrical engineering from Nagoya University, Nagoya, Japan, in 1992 and 1994, respectively.

He is currently a graduate student at Nagoya University, where he has been studying the high-current SF_6 arc interruption phenomena.

Yasunobu Yokomizu (M'91) was born in Aichi, Japan, on October 13, 1962. He received the B.S., M.S., and Ph.D. degrees in electrical engineering from Nagoya University, Nagoya, Japan, in 1985, 1987, and 1991, respectively.

He is now an Assistant Professor, in the Department of Electrical Engineering at Nagoya University. His main interests are in high-current arc physics and in applications of superconductors to electric power apparatus.

Dr. Yokomizu is a member of the IEE of Japan.

Motohiro Ishikawa was born in Aichi, Japan, on September 24, 1972. He received the B.S. degree in electrical engineering from Nagoya University, Nagoya, Japan, in 1994.

He is currently a graduate student at the Nagoya University, where he has been studying the high-current SF_6 arc interruption phenomena.

Toshiro Matsumura (M'95) was born in Wakayama, Japan, on May 1, 1951. He received the B.S., M.S., and Ph.D. degrees in electrical engineering from Nagoya University, Nagoya, Japan, in 1974, in 1976 and 1980, respectively.

He is now a Professor in the Department of Electrical Engineering at Nagoya University. He is currently involved in a study on an effective utilization of electrical energy and on high-current arc interruption phenomena.

Dr. Matsumura is a member of the IEE of Japan.

Yukio Kito (M'70–SM'92–F'94) was born in Aichi, Japan, on March 12, 1933. He received the B.S., M.S., and Ph.D. degrees in electrical engineering from Nagoya University, Nagoya, Japan, in 1955, 1957, and 1962, respectively.

He was a Professor at Nagoya University from 1974 to 1995. He is now a President of Toyota National College of Technology and an Emeritus Professor of Nagoya University.

Dr. Kito is a member of the IEE of Japan.